

Journal of Materials Chemistry C

Accepted Manuscript



This is an *Accepted Manuscript*, which has been through the Royal Society of Chemistry peer review process and has been accepted for publication.

Accepted Manuscripts are published online shortly after acceptance, before technical editing, formatting and proof reading. Using this free service, authors can make their results available to the community, in citable form, before we publish the edited article. We will replace this *Accepted Manuscript* with the edited and formatted *Advance Article* as soon as it is available.

You can find more information about *Accepted Manuscripts* in the [Information for Authors](#).

Please note that technical editing may introduce minor changes to the text and/or graphics, which may alter content. The journal's standard [Terms & Conditions](#) and the [Ethical guidelines](#) still apply. In no event shall the Royal Society of Chemistry be held responsible for any errors or omissions in this *Accepted Manuscript* or any consequences arising from the use of any information it contains.

Polyelectrolyte Multilayer-assisted Fabrication of p -Cu₂S/ n -CdS Heterostructure Thin Films Phototransistor

Ramphal Sharma,^{1,2,*†} Gangri Cai,^{2,3†} Dipak V. Shinde,² Supriya A. Patil,² Shaheed Shaikh,¹ Anil Vithal Ghule,² Rajaram S. Mane² and Sung-Hwan Han^{2,*†}

¹Thin Film and Nanotechnology Laboratory, Department of Physics, Dr. Babasaheb Ambedkar Marathwada University, Aurangabad 431004 (India)

²Inorganic-Nanomaterials Laboratory, Department of Chemistry, Hanyang University, Sungdong-Ku, Haengdang-dong 17, Seoul 133-791 (South Korea)

³Department of Applied Chemistry, Tianjin University of Technology, Tianjin 300384, People's Republic of China.

[†]These authors contributed equally to this work.

Abstract

We demonstrate meticulous fabrication of p -Cu₂S/ n -CdS heterojunction thin-films using a facile wet chemical approach. Ion exchange of Cu⁺ with Cd²⁺ is a serious problem while preparing Cu₂S/CdS multilayered thin films. We have addressed this issue here by employing polyelectrolyte multilayers on the surface of CdS, which completely prevents the corrosion of CdS, which in turn allowed us to fabricate heterostructured Cu₂S/CdS films. The formation of polyelectrolyte multilayers is monitored using cyclic voltammetry. The heterostructured films are characterized for their structure and morphology. We further employed these films as modified p -channel p -Cu₂S/ n -CdS thin-film phototransistor, where, n -CdS acts as electron transporting and hole-blocking layer, which extracts and grounds the photogenerated electrons. This device exhibited significant increase in photocurrent density (>75 times), drift mobility (>87 times), and good linearity without having to apply gate voltage, when compared to its individual component device.

*Authors to whom all correspondence can be addressed. E-mail: rps.phy@gmail.com (Ramphal Sharma, Prof.); Ph.:+91-9422793173; shhan@hanyang.ac.kr (Sung-Hwan Han, Prof.), Fax: +822-2299-0762. †These authors contributed equally to this work.

Introduction

Nanostructured thin film phototransistors are transistors in which the incident light intensity can modulate the charge-carrier density in the channel. Compared with conventional photodiodes, phototransistors enable easier control of light-detection sensitivity without problems such as the noise increment. However, scientific and technological advances in solid-state electronics should be achievable with the efficacy to fabricate and tailor solution-based semiconducting thin-films and electronically couple in a general way.^{1-5, 8} Thus, exploring and fabricating high performance semiconductor thin-films and their combinations using wet chemical route as an economic alternative (in terms of cost, reliability, availability, processability, driving energy etc.),¹⁻⁹ and employing them into devices with the expectation of new technologies, is a great challenge in contemporary science and has always attracted researchers. Among the solution-processed thin-film transistors (TFTs), organic TFTs have generated great interest because of their potential as a low-cost and light weight alternative,^{1, 4, 8} but their intrinsic physicochemical and optoelectronic properties decide their application scope. Earlier studies have demonstrated the significance of metal oxide semiconductors (ZnO, SnO₂, In₂O₃, etc.) and carbon nanotubes in fabricating photo and electrochemically stable TFTs,^{2, 10, 11} which were developed with the motivation to replace conventional silicon (polycrystalline and amorphous)-based TFTs by overcoming their limitations such as, low mobility, non-transparency, and high processing temperatures etc.^{2, 10} New semiconductors, chalcogenides³ and heterojunctions (junction field-effect transistors)⁸ are

also being explored as viable alternative to metal oxide semiconductors to overcome issues of gate leakage current and charge transfer efficiency. Chalcogenides semiconductors, with advantage of unique optoelectronic properties, higher mobility, ready availability, processability, and low cost, have gained acceptance over organic and conventional semiconductors in scientific and technological applications.⁹ Although, great progress in synthesizing different morphologies and bulk heterojunctions of II-VI (CdS, Cu₂S, CdSe, CdTe, etc.) chalcogenides is achieved,¹² gas phase deposition techniques have been the methods of choice for a long time despite the drawbacks of limited precursor materials and use of high cost vacuum facilities. As alternative approaches, several wet chemical routes have been developed, such as chemical bath deposition (CBD), layer by layer (LbL) deposition, electrodeposition, sol-gel, spin coating etc.^{3, 8, 9, 13} Recently, Mitzi *et al.*³ demonstrated an innovative approach for spin coating ultrathin (~50 Å) crystalline semiconducting SnS_{2-x}Se_x films and their application in field-effect transistors. However, LbL deposition of II-VI and III-VI bilayers of semiconductors by wet chemical route poses a great problem in controlling the ions exchange with the metal oxide and chalcogenide surfaces,¹⁴⁻¹⁷ when the first layer is immersed in the precursor solution for depositing subsequent layers.⁸ Hence, fabricating multilayer thin-films and heterojunctions addressing an important issue of possible ion exchanges and their protection remains a great challenge. Polyelectrolyte multilayer were used as nanostructure materials,⁷ but for the first time in this communication we report its application for fabricating multilayered chalcogenide thin-film structures as a unique approach by controlling and/or prohibiting ion transport through the engineering of cations-anions of polyelectrolyte layers. Although, *p*-Cu₂S/*n*-CdS system has been extensively investigated as a solar cell material between 60 s and 80 s and is revisited recently,¹⁸ its application as thin-film phototransistor (TFPTs) is yet to be explored. TFPTs, which integrate

optoelectronic properties combining light detection and signal magnification that realizes great functionality in a single device, are also explored with interest owing to their technological advantages over TFTs and photodiodes. With this motivation, the present study reports novel highly stable TFPT device design of Cu₂S/CdS heterojunction on the indium-tin-oxide (ITO) substrates, successfully fabricated with the aide of protective polyelectrolyte multilayers using modified wet chemical method. This device is found to exhibit higher photocurrent density than its individual component device.

Experimental

Thin film deposition: Aqueous solutions of CdCl₂·2H₂O (0.02 M, 25 mL) and NH₂CSNH₂ (0.03 M, 25 mL) were prepared separately in deionized (DI) water. The two solutions were mixed in a beaker and stirred constantly with pH maintained at ~11 by adding (2 mL min⁻¹) 27% aq. NH₄OH solution. CdS thin-films were deposited using CBD on pre-cleaned ITO substrates, which were immersed in the solution for 1 h with reaction bath temperature maintained at 80 °C. The dark-yellow coloured CdS thin-films were annealed at 150 °C in air for 1 h. Alternate layers of polyelectrolytes (PEI, 0.2 g in 100 mL) and (PAA, 0.2 g in 100 mL) as multilayers, denoted as (PEI/PAA)_n (n= 0.5, 1.5, 2.5, 3.5), were dip-coated on the ITO/CdS film at pH ~11 with 1 h of dipping time for each layer. Cu₂S films on ITO and as subsequent layer on ITO/CdS/(PEI/PAA)_{1.5} substrate were deposited using CBD with reaction time of 1 h, where, separately prepared aqueous solutions of CuSO₄·5H₂O (0.02 M, 50 mL), triethanolamine (TEA, 0.2 g in 50 mL) and NH₂CSNH₂ (0.02 M, 50 mL) were mixed in a beaker and stirred constantly with pH maintained at 11. The reaction bath temperature was maintained at 40 °C. TEA forms a Cu-metal complex and controls metal oxidation and ion deposition rate. The reaction between Cu⁺ and S²⁻ ions forming Cu₂S is confirmed from the solution colour transforming from blue to

dark-brown (10 min) and then golden-brown (transparent) after 1 h. The films were washed with DI water, annealed in air at 200 °C (1 h) and subjected to further characterization.

Characterizations:

The annealed samples were characterized by powder X-ray diffractometer (XRD, Siemens D-5005, Cu-K α 1 radiation, V = 40 kV and I = 100 mA), SEM (Hitachi S-4200), XPS (VG Multi Lab ESCA 2000 system), UV-Vis spectrometer (Cary 100, Japan), and photoluminescence spectrometer (Photon-counting spectrometer, ISS Inc.). Current density-voltage (*J-V*) characteristics of the fabricated TFPT devices were obtained in dark and by varying light intensity (10-100 mW cm⁻²) using Thermo Oriel Instruments. The ion-permeability study was performed using cyclic voltametry (CV) with anionic Fe(CN)³⁻₆ and cationic Ru(NH₃)³⁺₆ redox probe molecules²⁰. The sandwich layers (PEI/PAA)_{1.5} of the *p*-Cu₂S/*n*-CdS thin films annealed at 200⁰ 1h in air are analyzed using cations and anions spectrums of TOF-SIMS spectroscopy in the imaging modes analysis by conventional method. Optical image of *p*-Cu₂S/*n*-CdS TFPT was obtained by conventional method, when light (source light intensity 100 mW.cm⁻²) allowed in between the source and drain (5mm x 5mm) of the device.

Results and discussion

Modifying the electrodes with polyelectrolyte (cations-anions) develop charges on their surface through coulombic interactions with ions in solution, which prohibit ion-exchange reactions thereby protecting the chalcogenide semiconducting films from corrosion/dissolution.^[19] In continuation of this strategy, alternate layers of polyelectrolyte (PEI and PAA) were employed as ion protecting layers over pre-deposited CdS layer with the intention of prohibiting Cu⁺ ion exchange reactions during the subsequent growth of Cu₂S layer using alkaline CBD. **PEI and PAA have positive and negative ions** which play important role, such as; the positively charged

PEI layers prevent positively charged Cu^+ ions from the solution and attract the negatively charged S^{2-} ions in solution. On the other hand, the PAA layers stack with PEI layers to form compact multilayer structure. There for, Cu^+ ions in solution cannot physically bypass the compact PEI-PAA layers. Consequently, the Cu^+ ions in solution are unable to reach the CdS surface through the PEI and PAA multilayers or sandwich layers. Cyclic voltametry (CV) study monitoring ion-permeability (which is controlled by surface charge density i.e. amount of NH_3^+ groups) was used to optimize the pH~11 (supplementary data Fig. S1a) and the number of polyelectrolyte layers (**Fig. 1a**) to be employed.^[7, 20] Fig. 1a shows reduction in redox current of the cationic probe with increasing number of ion protective $(\text{PEI/PAA})_n$ ($n= 0.5, 1.5, 2.5, 3.5$ as number of bilayers, where $(\text{PEI/PAA})_{0.5}$ means a single PEI layer and $(\text{PEI/PAA})_{1.5}$ means PEI/PAA/PEI alternative layers and so on) layers on the ITO/CdS films with the pH maintained at ~11. Successive shift and decrease in redox current density in the cyclic voltammogram implies effective blocking of cation diffusion with $(\text{PEI/PAA})_n$ (n is 1.5 and above) as inset of Fig. 1a. Thus, $(\text{PEI/PAA})_{1.5}$ sandwich layers are used in fabricating highly stable $\text{Cu}_2\text{S/CdS}$ thin-film heterojunction and such sandwich layers are converted into cations-anions layers after air annealing at 200°C for 1 h. In the sandwich layers, the surface charge and structure of polyelectrolyte multilayers are the critical factors to control the ion permeability (protection) also after the annealing of thin-film heterojunction. Which is confirmed by Time-of-Flight Secondary Ion Mass Spectrometry (TOF-SIMS) study (supplementary data Fig. S1b and S1c).

The scanning electron microscopy (SEM) image (**Fig. 1b**) of $\text{Cu}_2\text{S/CdS}$ thin-film shows smooth surface with Cu_2S nanoparticles covering the entire CdS layer. SEM cross-section view of the film shows two distinct layers clearly indicating the thicknesses of CdS (~500 nm) and Cu_2S (~1000 nm) films (Fig. 1b inset). The composition of the films is confirmed from the

energy dispersive X-ray analysis (supplementary data Fig. S2). Quantitative elemental analysis shows the presence of elements in atomic percentages as Cd (25.5%), Cu (28.5%) and S (46.0%). The XRD (**Fig. 1c**) shows the presence of CdS (cubic phase, PDF 75-1546) and Cu₂S (orthorhombic phase, PDF-72-0617) structures. This justifies the composition of the Cu₂S/CdS thin-film heterojunction, which is further supported by X-ray photoelectron spectroscopy (XPS) (supplementary data Fig. S3). UV-Vis (supplementary data Fig. S4) and photoluminescence (PL) spectra (**Fig. 1d**) were recorded from Cu₂S/CdS thin-film heterojunction and Cu₂S film to study the optical properties and the contribution from Cu₂S film. Higher UV absorption in the 400-700 nm wavelength range is observed as a result of Cu₂S/CdS heterojunction formed at the interface confirming that it is not mere summation of absorptions from individual Cu₂S and CdS films. PL spectrum obtained from Cu₂S film shows strong emission around 425 nm (Fig. 1d). On the contrary, significant PL quenching by a factor of ~50 times is observed from Cu₂S/CdS thin-film heterojunction as a result of excited-state interactions between CdS and Cu₂S. The observed quenching represents the deactivation of the excited Cu₂S *via* energetically favoured electron transfer to CdS having lower conduction band as shown in the schematic (Fig. 1d inset).^[21] The cartoon image of CdS-polyelectrolyte-Cu₂S layers is shown in fig. 1e for more clarity and understanding.

TFPT devices were fabricated using gold metal contacts separated by 5 mm on the thin-film surfaces (Cu₂S/CdS and Cu₂S) working as a source and drain. The photo-illuminated area between the source and drain is assumed to be the virtual gate²² with ITO grounded in this system. The schematic of the fabricated *p*-Cu₂S/*n*-CdS TFPT device (device 1) design is shown as inset in **Fig. 2a**. The *J-V* measurements in dark and with varying light intensities (10-100 mW cm⁻²) obtained from device 1 show significant increase in photocurrent density (Fig. 2a) when

compared to dark, and individual Cu₂S TFPT device (device 2) (details in supporting data). The dark current densities (0 mW cm⁻²) in device 1 and device 2 are 8.5 and 0.51 mA cm⁻², but device 1 shows significantly higher photocurrent density (106.5 mA cm⁻²) when compared to device 2 (1.43 mA cm⁻²) with 100 mW cm⁻² light intensity at source voltage of 3.5 V, indicating about 75 times increase in photocurrent density by adding *n*-type layer in the device 1 structure. The observed photocurrent density is higher than reported for most organic TFPTs, metal oxide TFPTs, and chalcogenide semiconductor based TFPTs and others in this category.^{4, 8, 13, 23} This is attributed to the modified TPFT device design, which effectively separates the photogenerated charge carriers across the *p-n* junction *via* blocking the holes and at the same time transferring and grounding of electrons through CdS layer. This in turn increases the hole concentration and also facilitates its transport in the *p*-Cu₂S channel by minimizing possible hole-electron recombination. The process involves (a) the generation of excitons *via* the absorption of light; (b) the breaking of excitons to electrons and holes followed by transfer of electron to ground through CdS; and (c) the flow of mobile carriers (holes in this case) in the *p*-channel Cu₂S layer of the phototransistor *via* source–drain bias. From Fig. 2a, it is also observed that the saturation in photocurrent density is achieved at as low as 3.5 V, which is important from device application and technology point of view.

Plot of photocurrent density as a function of light intensity obtained from device 1 shows good linearity in the range 0-100 mW cm⁻² as compared to low photocurrent density and poor linearity (**Fig. 2b** and inset with schematic) observed in device 2 of Cu₂S only system. Our results imply that, the light illumination area in between the source and drain acting as a generated small area virtual gate controls the photocurrent density and the device operation. The generated small area virtual gate was (about 100 x 100 μm²) measured from the light activated area, which is

confirmed by optical image photograph, when light is allowed to fall in between the source and drain of the TFPTs devices (supporting data Fig.11b)). The drift mobility μ , which is a function of carrier concentration, is defined as the velocity v of the charge carriers divided by the electric field E .²³

$$\mu = \frac{v}{E}, \text{ where, } v = \frac{I_{DS}}{WQ}, E = \frac{V_{DS}}{L} \quad (1)$$

I_{DS} is photocurrent obtained at specific source voltage V_{DS} (3.5 V in this case), Q is induced charge per channel area, W (width, 5 mm) and L (length 5 mm) of the TFPT channel. Plot of drift mobility μ as a function of light intensity (0-100 mW cm⁻²) calculated from the J - V data of devices 1 and 2 are presented in Fig. 2b and its inset, respectively. Good linearity in drift mobility is noted in device 1 (Fig. 2b) when compared device 2 (Fig. 2b inset). It is interesting to note that the drift mobility at dark current in device 1 (36.2 cm² V⁻¹s⁻¹) is ~8 times higher than in device 2 (4.6 cm² V⁻¹s⁻¹) and it increases on photo-illumination with light intensity (100 mW cm⁻²) to 1190 and 15.6 cm² V⁻¹s⁻¹, respectively, which is ~76 times higher than in device 2 (Cu₂S only TFPT). This is attributed to the synergistically enhanced hole concentration by effectively draining the electron through the grounded n -CdS layer and at the same time minimizing the hole-electron recombination, justifying the observed increase in photocurrent density^{21, 23} when compared to its individual component device (Cu₂S only TFPT) and ungrounded n -CdS layer system (details in supporting information data).

Conclusions

In summary, we have demonstrated p -Cu₂S/ n -CdS heterojunction thin-films in ambient atmospheric conditions using a simple chemical bath deposition (CBD) technique; where

polyethyleneimine (PEI) and polyacrylic acid (PAA) play a crucial role as protecting layers. Polyelectrolyte multi-layers block the Cu^+ ion diffusion making it possible to deposit Cu_2S on CdS layer without exchanging Cd^{2+} ions, thereby avoiding the damage to CdS layer during the CBD process. The $p\text{-Cu}_2\text{S}/n\text{-CdS}$ thin-film heterojunction presents valuable structural and chemical properties, excellent optical properties and $J\text{-}V$ characteristics essential for the fabrication of simple and economic phototransistor working in visible light. Further, we fabricate a novel modified p -channel $p\text{-Cu}_2\text{S}/n\text{-CdS}$ TFPT. The significance of the present work lies in the TFPT device design, which is a unique structure where, $n\text{-CdS}$ as electron transporting and hole-blocking layer, extracts and grounds the photogenerated electrons minimizing the carrier traps or charge recombination in $p\text{-Cu}_2\text{S}$ channel. Thereby increasing the hole concentration and mobility in the $p\text{-Cu}_2\text{S}$ channel. This device exhibits significant increase in photocurrent density (>75 times), drift mobility (>87 times), and good linearity without having to apply gate voltage, when compared to its individual component device, which is attributed to the modified design of $p\text{-Cu}_2\text{S}/n\text{-CdS}$ heterojunction TFPT. From practical point of view, the modified $p\text{-}n$ junction TFPT device is designed for the first time by low cost wet chemical method using protective polyelectrolyte multilayers and is expected to stimulate further experimental and theoretical investigations along these lines. This approach will become a powerful strategy for fabricating ordered inorganic heterostructured thin-films, with different but selective chemical compositions using wet chemical route, which are otherwise difficult to grow. We anticipate that our novel $p\text{-}n$ junction based TFPT design with improved performance would be the starting point for new genera of TFPT, TFT, and solar cell. Further improvements in the device design, changing compositions and fabricating thin-film phototransistors to study their characteristics properties are in progress.

Acknowledgements

This work was supported by Nano R&D program through KOSEF funded by the Ministry of Education, Science and Technology (M1080300131008M 030031010) and Brain Korea 21. R. S. is thankful for the Brain Pool Fellowship (Korea), Visiting Professor at Hanyang University and to Dr. B.A.M. University, Aurangabad, India for the study leave.

References

- [1] a) S. R. Forrest, *Nature* **2004**, *428*, 911. b) C. R. Kagan, D. B. Mitzi, C. D. Dimitrakopoulos, *Science* **1999**, *286*, 945. c) H. E. Katz, A. J. Lovinger, J. Johnson, C. Kloc, T. Siegrist, W. Li, Y. Y. Lin, A. Dodabalapur, *Nature* **2000**, *404*, 478.
- [2] J. F. Wager, *Science* **2003**, *300*, 1245.
- [3] D. B. Mitzi, L. L. Kosbar, C. E. Murray, M. Copel, A. Afzali, *Nature* **2004**, *428*, 299.
- [4] C. D. Dimitrakopoulos, P. R. L. Malenfant, *Adv. Mater.* **2002**, *14*, 99.
- [5] a) I. Gur, N. A. Fromer, M. L. Geier, A. P. Alivisatos, *Science* **2005**, *310*, 462. b) M. A. Green, K. Emery, Y. Hishikawa, W. Warta, *Prog. Photovolt: Res. Appl.* **2009**, *17*, 85.
- [6] T. Kyratsi, K. Chrissafis, J. Wachter, K. M. Paraskevopoulos, M. G. Kanatzidis, *Adv. Mater.* **2003**, *15*, 1428.
- [7] X. Shi, M. Shen, H. Möhwald, *Prog. Polym. Sci.* **2004**, *29*, 987.

- [8] a) S. Cho, J. Yuen, J. Y. Kim, K. Lee, A. J. Heeger, S. Lee, *Appl. Phys. Lett.* **2008**, *92*, 063505. b) X. Liu, Y. Guo, Y. Ma, H. Chen, Z. Mao, H. Wang, G. Yu, and Y. Liu, *Adv. Mater.* **2014**, (DOI: 10.1002/adma.201306084), 1
- [9] R. S. Mane, C. D. Lokhande, *Mater. Chem. Phys.* **2000**, *65*, 1.
- [10] S. Y. Ju, A. Facchetti, Y. Xuan, J. Liu, F. Ishikawa, P. D. Ye, C. W. Zhou, T. J. Marks, D. B. Janes, *Nature Nanotechnol.* **2007**, *2*, 378.
- [11] a) S. Kim, S. Ju, J. H. Back, Y. Xuan, P. D. Ye, M. Shim, D. B. Janes, S. Mohammadi, *Adv. Mater.* **2009**, *21*, 564. b) S.E. Ahn, I. Song, S. Jeon, Y. W. Jeon, Y. Kim, C. Kim, B. Ryu, J.H. Lee, A. Nathan, S. Lee, G. T. Kim, and U.I. Chung, *Adv. Mater.* **2012**, *24*, 2631–2636. c) S.E. Ahn, S. Jeon, Y. W. Jeon, C. Kim, M.J. Lee, C.W. Lee, J. Park, I. Song, A. Nathan, S. Lee, and U.I. Chung, *Adv. Mater.* **2013**, *25*, 5549–5554.
- [12] a) S. Kumar, T. Nann, *Small* **2006**, *2*, 316. b) W. T. Yao, S. H. Yu, *Adv. Funct. Mater.* **2008**, *18*, 3357. c) X. Wang, J. Zhuang, Q. Peng, Y. D. Li, *Nature* **2005**, *437*, 121. d) D. V. Talapin, J. H. Nelson, E. V. Shevchenko, S. Aloni, B. Sadtler, A. P. Alivisatos, *Nano Lett.* **2007**, *7*, 2951.
- [13] F. Y. Gan, I. Shih, *IEEE Trans. Electron Devices* **2002**, *49*, 15.
- [14] J. E. Lilienfeld, in *US patent 1745175*, USA, **1926**.
- [15] F. Pfisterer, *Thin Solid Films* **2003**, *431*, 470.

- [16] K. W. Boer, *Phys. Rev. B* **1976**, *13*, 5373.
- [17] A. M. Aldhafiri, G. J. Russell, J. Woods, *Semiconductor Sci. Technol.* **1992**, *7*, 1052.
- [18] Y. Wu, C. Wadia, W. L. Ma, B. Sadler, A. P. Alivisatos, *Nano Lett.* **2008**, *8*, 2551.
- [19] Y. Kim, G. Cai, W. Lee, K. Hyung, B. W. Cho, J. K. Lee, S. H. Han, *Curr. Appl. Phys.* **2009**, *9*, S65.
- [20] M. K. Park, S. X. Deng, R. C. Advincula, *J. Am. Chem. Soc.* **2004**, *126*, 13723.
- [21] a) P. V. Kamat, *J. Phys. Chem. C* **2008**, *112*, 18737. b) K. Rajeshwar, N. R. de Tacconi, C. R. Chenthamarakshan, *Chem. Mater.* **2001**, *13*, 2765.
- [22] K. Lee, K. T. Kim, K. H. Lee, G. Lee, M. S. Oh, J. M. Choi, S. Im, S. Jang, E. Kim, *Appl. Phys. Lett.* **2008**, *93*, 193514.
- [23] K. Ryu, I. Kymissis, V. Bulovic, C. G. Sodini, *IEEE Electron Devices Lett.* **2005**, *26*, 716.

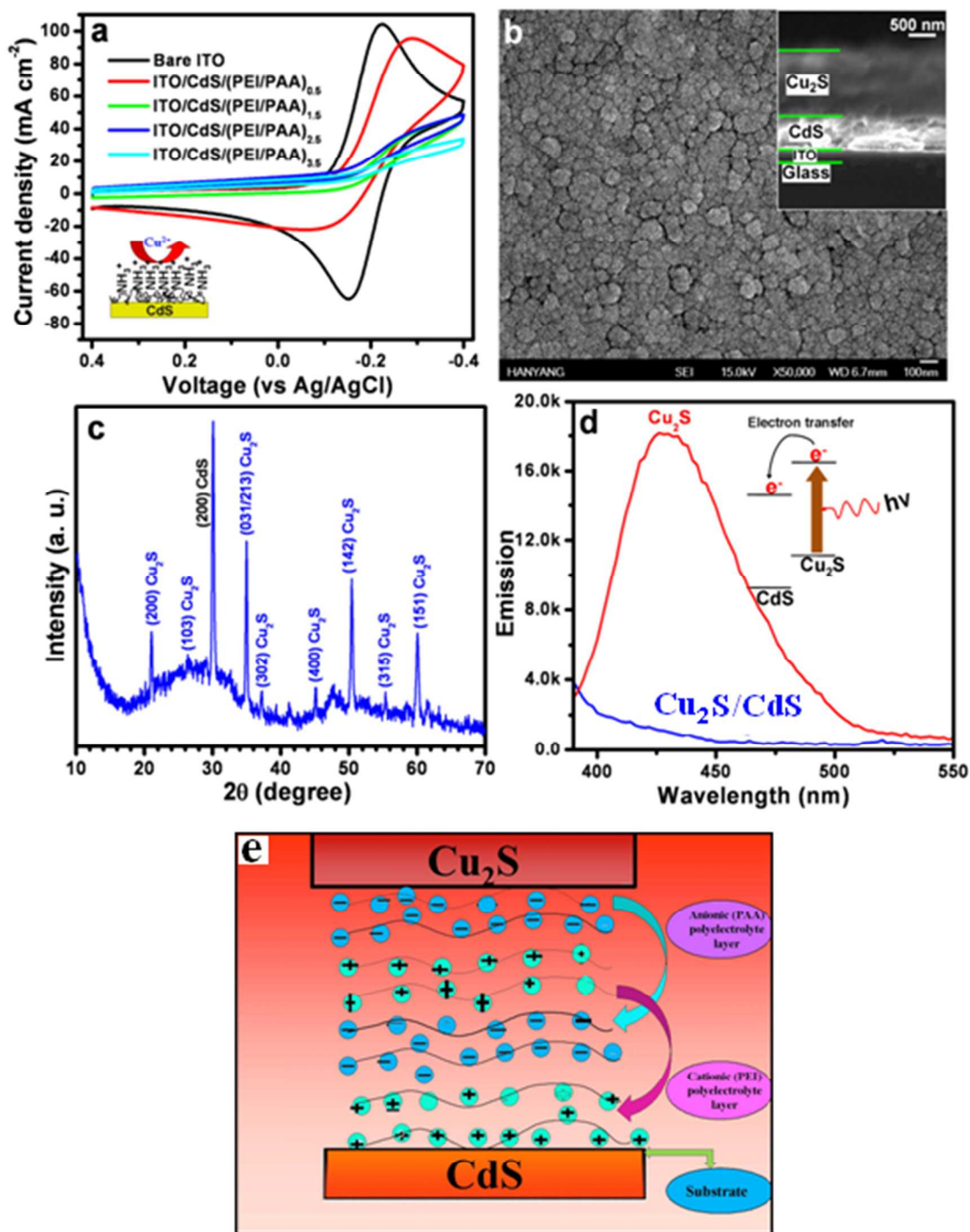


Figure 1. a) Cyclic-voltammograms obtained using ITO/CdS/(PEI/PAA)_n (n= 0.5, 1.5, 2.5, 3.5) layers and at a fixed pH ~11 to optimize the best condition for blocking Cu⁺ cations during the Cu₂S deposition. b) SEM images obtained from Cu₂S/CdS thin-film after annealing. Inset is

SEM cross-section view of the film showing CdS and Cu₂S film thicknesses. c) XRD pattern of the Cu₂S/CdS thin-film; the reflection indices are shown in parenthesis. d) Photoluminescence (PL) spectra obtained from Cu₂S/CdS thin-film in comparison with Cu₂S film. Inset is the schematic of observed PL quenching. e) A cartoon image showing the CdS, polyelectrolytes and Cu₂S layers. Polyelectrolyte helps to prevent the Cu⁺ exchange reaction.

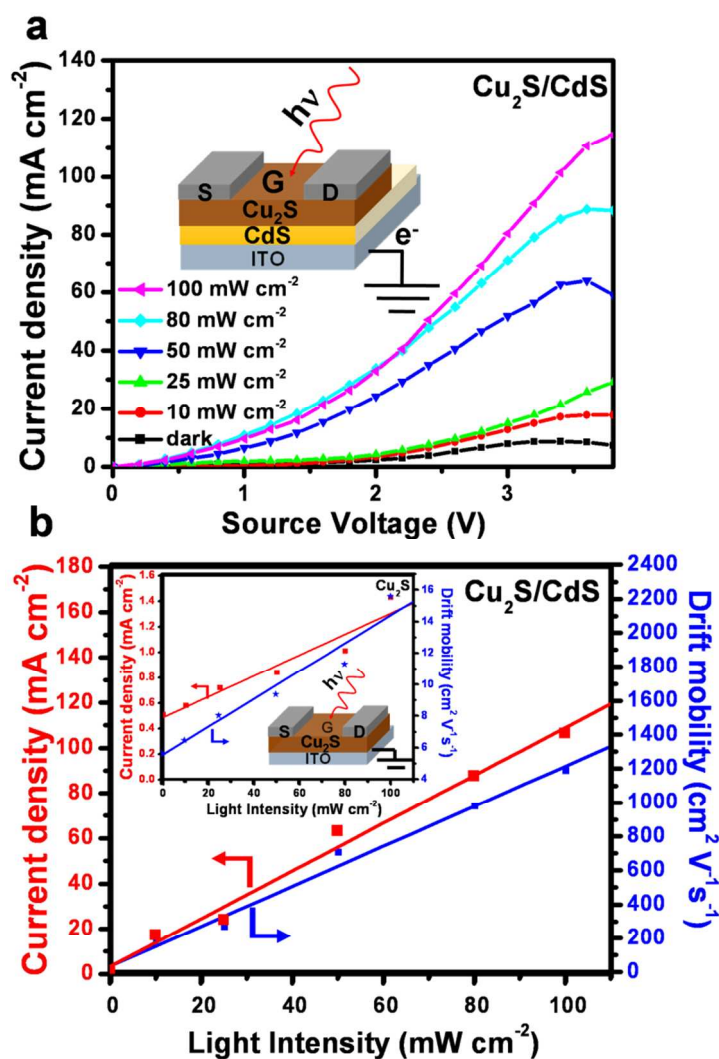


Figure 2. a) *J-V* plots in dark and with varying light intensities (10-100 mW cm⁻²) obtained from *p*-Cu₂S/*n*-CdS TFPT device showing increase in photocurrent density as a function of light intensity. Inset shows the schematic of *p*-Cu₂S/*n*-CdS TFPT device design. b) Plot of

photocurrent density (left y-axis scale) and drift mobility μ (right y-axis scale) calculated from J - V data at source voltage of 3.5 V as a function of light intensity (0-100 mW cm⁻²) obtained from p -Cu₂S/ n -CdS TFPT device showing good linearity. Inset shows plot of photocurrent density (left y-axis scale) and drift mobility μ (right y-axis scale) extracted from J - V data at source voltage of 3.5 V as a function of light intensity obtained from Cu₂S TFPT device along with the schematic of the device design.